Local work function analysis of Pt/TiO_2 photocatalyst by Kelvin probe force microscope

K Hiehata[1], A Sasahara[1,2] and H Onishi[1]

[1]Department of Chemistry, Faculty of Science, Kobe University, Nada-ku, Kobe 657-8501, Japan

[2]Japan Science and Technology Agency, Kawaguchi, Saitama 332-0012, Japan

E-mail: sasahara@kobe-u.ac.jp.

Abstract. Nanometer-sized Pt clusters were prepared on a TiO_2(110)-(1×1) surface, and lateral distribution of work function was examined by using a Kelvin probe force microscope. Local work function on the Pt clusters was smaller than that on the surrounding TiO_2 surface. Assuming that the dipole moments which perturb work function are produced by uneven electron distribution, the decrease of the work function indicates electron transfer from the clusters to the TiO_2 surface. After decomposition of pivalate anions on the surfaces by UV irradiation, the work function increased on some Pt clusters. It is known that holes photoexcited in TiO_2 attach to pivalate anions to cause a decomposition reaction. Hence the increase of the observed work function by UV irradiation can be ascribed to the trapping of the accompanying electrons to the Pt clusters.

Introduction

Platinum is a highly efficient cocatalyst for photocatalytic reactions on titanium dioxide (TiO_2) [1,2]. Improved catalytic performance is attributed to electron trapping by nanometer-sized Pt clusters as well as to their catalytic activity. The electrons transferred to the Pt clusters are separated from accompanying holes, and the electron-hole recombination is suppressed. Thus the electrons and holes induce photocatalytic processes with high efficiency. The electron trapping by Pt clusters has been proposed on the basis of experimental results indicating depletion of photogenerated electrons in the TiO_2. The conductance of the TiO_2 under UV irradiation, which is proportional to the free electron density, decreases with the amount of loaded Pt [3]. Time-resolved visible [4] and infrared [5,6] absorption spectroscopy studies have revealed that the Pt-loading enhances decay rate of electrons photogenerated in the conduction band of the TiO_2.

In this work, visualization of the trapping of photogenerated electrons by the Pt clusters was attempted. Performance of Pt/TiO_2 photocatalysts was sensitive to the size and surface density of the clusters [7,8], which indicates that the capability of trapping electrons was different between clusters. Identification of clusters which efficiently trap electrons offers a way to optimize the catalytic performance. With the assumption that unevenly distributed electrons induce dipole moments and modify work function, the distribution of electrons was examined from work function maps obtained using a Kelvin probe force microscope (KFM) [9,10].

A model of the Pt/TiO_2 photocatalyst was prepared using a (110) surface of rutile TiO_2. The accepted structure of the nonreconstructed (110) surface [11] is presented in **Figure 1**. The topmost O atoms are bound to two 6-fold-coordinated Ti atoms in a bridging coordination and form rows along the [001] direction. Between the O atom rows, Ti atoms coordinated to five O atoms are exposed. A pivalic acid molecule ($(CH_3)_3CCOOH$) dissociates to a pivalate ($(CH_3)_3CCOO^-$) and a hydrogen atom on the (1×1) surface at room temperature as shown in reaction (1) [12,13]. The pivalate is anchored to two 5-fold-coordinated Ti atoms with the OCO plane normal to the surface and forms a stable monolayer with a (2×1) periodicity. An accompanying hydrogen atom forms a surface hydroxyl group on a bridging O atom.

$$(CH_3)_3CCOOH + Ti^{4+}\text{-}O^{2-}\text{-}Ti^{4+} \rightarrow (CH_3)_3CCOO^- + Ti^{4+}\text{-}OH^-\text{-}Ti^{4+} \quad (1)$$

Ultraviolet light irradiation of the pivalate-covered surface in a vacuum induced desorption of CO_2, isobutene ($(CH_3)_2C=CH_2$), and isobutane ($(CH_3)_3CH$) [14-16] at 300 K, which was a lower temperature than

where the pivalates are thermally desorbed [17]. The desorbed species indicated decarboxylation of the pivalate to *tert*-butyl radical ($(CH_3)_3C$), reaction (3), and was induced by hole h^+ produced by band-gap excitation of the TiO_2 (2).

$$TiO_2 + h\nu \rightarrow TiO_2 + h^+ + e^- \quad (2)$$

$$(CH_3)_3CCOO^- + h^+ \rightarrow (CH_3)_3C + CO_2 \quad (3)$$

The 6-fold-coordinated Ti atoms bound to the hydroxyl group were proposed as traps for the accompanying electrons (4) [16]. The signal intensity assignable to the Ti^{3+} in electron energy loss spectra increased with the irradiation time and reduced with post-exposure to O_2. Faint spots assignable to the OH group bound to Ti^{3+} group disappeared after the O_2 dose in scanning tunneling microscope (STM) images (5).

$$Ti^{4+}\text{-}OH^-\text{-}Ti^{4+} + e^- \rightarrow Ti^{3+}\text{-}OH^-\text{-}Ti^{4+} \quad (4)$$

$$Ti^{3+}\text{-}OH^-\text{-}Ti^{4+} + 1/2O_2 \rightarrow Ti^{4+}\text{-}O^{2-}\text{-}Ti^{4+} + H_2O \quad (5)$$

The photodecomposition of the pivalate (3) stopped before the pivalate monolayer was exhausted. When the surface 6-fold-coordinated Ti atoms were occupied by photogenerated electrons, the reaction (3) became competitive with the recombination of the photogenerated electrons and holes (6).

$$h^+ + e^- \rightarrow \text{heat} \quad (6)$$

The photodecomposition of the pivalates on the TiO_2(110) surface was improved by Pt-loading [18]. The decomposition rate of the pivalates was enhanced as the amount of Pt increased, which was attributable to the electron trapping by the Pt clusters.

Experimental section

The KFM is based on a noncontact atomic force microscope (NC-AFM) [19], and shows the topography and the work function map of the sample surface simultaneously. The NC-AFM detects a weak attractive force working between the probe and sample to regulate the probe-sample separation. A cantilever with a tip at one end is oscillated at its resonant frequency (f_0), and the attractive force perturbing the oscillation is monitored as a frequency shift of the cantilever oscillation (Δf). In the KFM measurement, the cantilever is used like a reference electrode of a Kelvin probe method [20]. The tip and sample surface form a capacitor, and the contact potential difference (CPD) between the tip and sample causes electrostatic interaction. The electrostatic interaction is derived as an additional oscillation component by modulating the sample bias

voltage (V_s) by AC voltage. The offset DC voltage which minimizes the electrostatic component corresponds to the CPD. The obtained CPD map shows a local work function distribution. Here we use "local work function" to definitely show the direction of the CPD shift. Some previous studies presented work function maps with an atom-scale contrast [10,21-24].

All experiments were performed using an ultra-high vacuum STM/NC-AFM system (JSPM4500A, JEOL) at room temperature. The microscope is in a chamber separated from a sample preparation chamber by a gate valve. The preparation chamber is equipped with an ion sputtering gun (EX03, Thermo) and low energy electron diffraction optics (BDL600, OCI). The base pressure of the system was 2×10^{-8} Pa.

Conductive Si cantilevers with an f_0 of 300 kHz and force constants of 14 N/m (NCS12, MikroMasch) were used as a probe. In the KFM measurement, the peak-to-peak amplitude and the frequency of the modulation AC voltage were 2 V and 2 kHz. The modulated signal was extracted from the oscillation signal by a lock-in amplifier (LI5640, NF). The DC offset voltage was regulated by a KFM controller (TM-Z50241, JEOL). Empty-state STM images were acquired in a constant current mode by using the cantilever as a probe.

The TiO_2(110) surface was cleaned by repetition of Ar-ion sputtering and annealing at 1100 K. A mechanically-polished TiO_2(110) wafer (Shinko-sha, $7\times1\times0.3$ mm^3) was supported on a Si wafer ($7\times1\times0.5$ mm^3) which was used as a resistive heater. The temperature of the sample monitored with an infrared pyrometer (TR630, Minolta) was possibly overestimated because the temperature of the Si wafer was measured through the transparent sample wafer. Platinum was evaporated from a heated Pt wire (99.98%, Nilaco) outgassed beforehand, and the surface was subsequently annealed to grow the clusters. The pressure increase during the evaporation was less than 8.0×10^{-8} Pa. Pivalic acid was degassed by freeze-pump-thaw cycles, and introduced into the preparation chamber through a leak valve. A 300W Xe arc lamp was used as an UV light source for decomposition of the pivalate. Ultraviolet light of 250-390 nm wavelengths was introduced to the chamber through a heat filter. The light flux at the surface was 10 Wm^{-2}.

The images taken with 512×512 data points are presented without filtering. The geometrically higher areas are shown as brighter areas in the topography, and areas with a larger work function are shown as brighter areas in the work function maps.

Results and discussions

Figure 2 shows a sequence of STM images of the TiO_2 surfaces which were obtained at each stage of the experiment. Image **(a)** shows the sputter-annealed TiO_2(110) surface. The surface consists of atomically flat terraces separated by monoatomic steps. The bright rows running in the [001] direction in the terraces correspond to the sites of the 5-fold-coordinated Ti atoms. At positive sample bias voltage, electrons tunnel into the 3d-derived states of the 5-fold-coordinated Ti atoms [25].

High Pt-loaded and low Pt-loaded TiO_2 surfaces were prepared. Low-loading of Pt was performed by 1 minute exposure of the TiO_2(110) surface to the Pt vapor followed by annealing at 1050 K for 10 s to reduce Pt adatoms by aggregation and/or desorption. Image **(b)** shows the obtained low-loaded surface. Bright particles with diameters of 1-2 nm and heights of 0.2-0.4 nm can be seen. The number density of the particles was 1×10^{16} m^{-2}. Ten minute Pt evaporation and subsequent annealing at 830 K for 20 min was employed to prepare a high Pt-loaded surface. The diameters and number density of the bright particles increased to 3-4 nm and 4×10^{16} m^{-2} as shown in image **(c)**. The heights were 0.2-0.4 nm and comparable to those of the particles in the low-loaded surface. The bright particles are assignable to Pt clusters from the increase of their sizes dependent on the exposure time to the Pt source. The formation of nanometer-sized Pt clusters was consistent with that of previous reports for the Pt-evaporated TiO_2(110) surfaces [18,26,27]. The numbers of the Pt atoms included in images **(b)** and **(c)** were estimated to be 300 and 4000, respectively, assuming a cylindrical shape and atom density in Pt metal, 6.6×10^{28} m^{-3}, for the clusters. The number density of the Pt atoms was proportional to the evaporation time. Encapsulation of the Pt clusters by TiO_x species [28] was unlikely, because the size and shape of the Pt clusters did not change after vacuum-annealing.

Images **(d)** and **(e)** are the low-loaded and high-loaded surfaces exposed to 900 L of pivalic acid gas, respectively. The spots arranged in a (2×1) periodicity on the terraces are pivalates. Dark patches indicated by arrows are the vacant sites where pivalates were not adsorbed. The number ratio of the pivalates to the bridge sites of two 5-fold-coordinated Ti atoms was 93% in image **(d)** and 86% in image **(e)**. Bright spots which appeared on the Pt clusters are presumably pivalates because their image height and diameter are comparable to those of the adsorbed pivalate on the TiO_2 portion.

Image **(f)** shows the low-loaded surface irradiated by UV light for an hour after the pivalate adsorption.

The pivalates on the terraces decreased, and the residing pivalates partly retained the (2×1) arrangement. Seventy percent of the adsorption sites in image **(f)** were occupied by the pivalates. Hence, the ratio of the removed pivalate from the low-loaded surfaces was estimated to be 25% from images **(d)** and **(f)**. Since the adsorbed pivalate is immobile on the (1×1) surface [15], the random distribution of the vacant sites indicates non-site-specific reaction of the pivalates. The image obtained on the high-loaded surface after photodecomposition of the pivalates by 2 hours irradiation is shown in **(g)**. The pivalates were observed at 61% of the adsorption sites, and 29% of the pivalates were removed from the high-loaded surface. Bright spots on the Pt clusters were not observed as shown in the inset of image **(g)**.

Figures 3(a) and **(b)** are topographic images (left column) and simultaneously obtained work function maps (right column) of the low-loaded and high-loaded surfaces which are not covered with pivalates. The bright particles marked by arrowheads in the topography are Pt clusters. Strings extending in the [001] direction on the low-loaded surface are Ti_2O_3 rows. The location of the clusters marked with an arrowhead are depressed in the work function maps, i.e., the work function on the clusters is smaller than that on the surrounding TiO_2 surfaces. Panel **(c)** is a schematic drawing of the work function map contrast. The work function decrease on the Pt clusters indicates that the dipole moments directed to the vacuum side were formed by electron transfer from the clusters to the substrate. The direction of the electron transfer indicated by the work function measurement is opposite to that predicted from work function of the bulk TiO_2 (5.3 eV [29]) and Pt (5.6 eV [30]). This suggests that physical and chemical properties of the nanometer-sized Pt clusters are perturbed from those of the bulk Pt. It is likely that the original neutral Pt atoms donated electrons to the cationic Ti atoms on the TiO_2 surface [21]. The work function difference between the individual Pt clusters and surrounding TiO_2 surface is plotted in graph **(d)** as a function of the cluster-TiO_2 interface area. A circle interface was assumed, and the diameters of the circles were determined from the cross sections of the topography. Uneven work function decrease on the clusters with approximately an equal interface area was possibly due to nonuniform atomistic structure at the cluster-TiO_2 interface.

Sets of topography and work function maps of the pivalate-covered surfaces are shown in **Fig. 4**. In both the topographies of the **(a)** low-loaded and **(b)** high-loaded surfaces, the Pt clusters were observed as bright particles, while adsorbed pivalates were not resolved. Compared to the pivalate-free surfaces, the work

function decrease on the Pt clusters was suppressed as illustrated in panel **(c)**. In addition, the average work function became smaller by 0.8 eV. It is illustrated in graph **(d)** how these features appeared on the pivalate-covered surfaces.

The work function perturbation which reflected the surface dipole moment originated from the pivalate adsorption. The adsorbed pivalate has an intrinsic dipole moment directed to the vacuum side due to the COO group polarized as $O^{\delta-}$-$C^{\delta+}$-$O^{\delta-}$ [31]. It is likely that the pivalates are anchored on the Pt clusters via COO group on the analogy of formate ($HCOO^-$) [32] and acetate (CH_3COO^-) [33] on Pt(111) surface. The intrinsic dipole moment contributes to the work function decrease equivalently on the TiO_2 surface and the Pt clusters. Another dipole moment formed at the pivalate-surface interface by electron transfer accompanying bond formation is a possible cause of the suppressed work function. The cationic Ti atom receives more electrons from the anionic pivalate compared to neutral Pt atoms. The pivalate-TiO_2 interface is more polarized, and the work function on the TiO_2 surface is more reduced than that on the Pt clusters. Dependence of the molecule-induced surface dipole moment on substrate material has been reported on a benzoic acid (C_6H_5COOH) molecule adsorbed on an indium-tin oxide and aluminum film [34].

Topography (left column) and work function maps (right column) obtained after the photodecomposition of the pivalates are presented in **Fig. 5**. Platinum clusters and increased vacant sites are visible in the topographic images. On the low-loaded surfaces, the number of Pt clusters showing larger work function than the surroundings increased noticeably. The panel **(c)** represents the change of the work function. The work function difference between the clusters and pivalate-covered TiO_2 surface is displayed in graph **(d)**. Thirty four percent of the clusters (15 out of 44) on the low-loaded surfaces showed a larger work function than that of the pivalate-covered TiO_2 surface, while the work function of the clusters on the high-loaded surfaces was smaller than that on the surroundings. The dispersed work function difference for the high-loaded surface is due to the fluctuated work function on the TiO_2 surface possibly caused by vacant areas.

One possible cause of the positive work function shift is the electron transfer from the TiO_2 substrate to the Pt clusters, which increases dipole moments directed to the substrate side. The number of trapped electrons after UV irradiation was equivalent to that of the desorbed pivalates, and is estimated to be 6×10^{17} m^{-2} on the low-loaded surface and 7×10^{17} m^{-2} on the high-loaded surface from the STM images. The

number density of the 6-fold-coordinated Ti atoms was 5×10^{18} and 3×10^{18} m^{-2} on the low-loaded and high-loaded surfaces, respectively. Here we assume that equivalent electrons were trapped at the Pt clusters on both surfaces. The Pt atoms at the cluster-TiO_2 interfaces are positively-charged after evaporation, and likely receive electrons. The low-loaded surfaces include fewer Pt atoms facing the interfaces than the high-loaded surfaces. The distribution of the electrons per one Pt atom is therefore larger on the low-loaded surfaces. The number density and/or strength of dipole moment directed to the vacuum side is more enhanced on the smaller clusters, which leads to distinct positive work function shift [26].

The dipole moment originating from adsorbates on the clusters is another factor to be considered. The work function on the clusters becomes larger when the pivalates are desorbed from the clusters. However, the work function increase was observed particularly on small clusters, which cannot be explained by the pivalate desorption independent of cluster size. Isobutene, isobutane, and carbonaceous species are possible adsorbates formed during the photodecomposition of the pivalates. The adsorption of these species reduce the work function on the clusters based on the analogy of the propane and propene adsorbed on a Pt(111) surface [35]. Carbon dioxide would not be stabilized on the cluster. No adsorbed CO_2 molecules were observed in the STM images obtained during CO oxidation on Pt(111) surface at 247 K [36]. Adsorption of residual H_2O and OH group from the H_2O is not likely at room temperature [37]. Hydrogen adatoms probably reduce the work function on the Pt clusters. The work function of Pt single crystal surfaces was reduced by the H adatoms [38,39]. Thus it is unlikely that the adsorbate contributes to the positive work function shift on the Pt clusters.

Summary

The work function of Pt-evaporated TiO_2(110) surfaces was examined by using KFM. Work function increase was observed on some Pt clusters after photodecomposition of pivalate anions. This suggests that the electron transfer coupled with the surface pivalate reaction can be detected by using the KFM. Future detailed studies of the electron trapping capability of the clusters will provide a basis for controlling photocatalytic performance.

Acknowledgements

The present work was supported by Core Research for Evolutional Science and Technology (CREST) from the Japan Science and Technology Agency (JST) and a Grant-in-Aid for Scientific Research in Priority Area “Molecular Nano Dynamics ” from the Ministry of Education, Culture, Sports, Science and Technology.

References

[1] Anpo M 2004 *Bull. Chem. Soc. Jpn.* **77** 1427

[2] Linsebigler A L, Lu G. and Yates J T Jr. 1995 *Chem. Rev.* **95** 735

[3] Disdier J, Herrmann J-M and Pichat P 1983 *J. Chem. Soc., Faraday Trans. I* **79** 651

[4] Furube A, Asahi T, Masuhara H, Yamashita H and Anpo M 2001 *Chem. Phys. Lett.* **336** 424

[5] Iwata K, Takaya T, Hamaguchi H, Yamakata A, Ishibashi T, Onishi H and Kuroda H 2004 *J. Phys. Chem. B* **108** 20233

[6] Yamakata A, Ishibashi, T and Onishi H 2003 *J. Mol. Catal. A: Chem.* **199** 85

[7] Sun B, Vorontsov A V and Smirniotis P G 2003 *Langmuir* **19** 3151

[8] Ohtani B, Iwai K, Nishimoto S and Sato S 1997 *J. Phys. Chem.* **101** 3349

[9] Nonnenmacher M, O'Boyle M P and Wickramasinghe H K 1991 *Appl. Phys. Lett.* **58** 2921

[10] Kitamura S and Iwatsuki M 1998 *Appl. Phys. Lett.* **72** 3154

[11] Diebold U 2003 *Surf. Sci. Rep.* **48** 53

[12] Sasahara A, Uetsuka H and Onishi H 2001, *Surf. Sci.* **481** L437

[13] Sasahara A, Pang C L and Onishi H 2006 *J. Phys. Chem.* **110** 4751

[14] White J M and Henderson M A 2005 *J. Phys. Chem. B* **109** 12417

[15] Uetsuka H, Onishi H, Henderson M A and White J M 2004 *J. Phys. Chem.* **108** 10621

[16] Henderson M A, White J, Uetsuka H and Onishi H 2003 *J. Am. Chem. Soc.* **125** 14974

[17] White J M, Szanyi J and Henderson M A 2004 *J. Phys. Chem. B* **108** 3592

[18] Uetsuka H, Pang C, Sasahara A and Onishi H 2005, *Langmuir* **21** 11802

[19] Morita S, Wiesendanger R and Meyer E 2002 *Noncontact Atomic Force Microscopy* (Berlin: Springer)

[20] Yates J T Jr. *Experimental Innovations in Surface Science* 2002 (Berlin: Springer) p 424

[21] Sasahara A, Pang C L and Onishi H 2006 *J. Phys. Chem. B* **110** 13453

[22] Sasahara A, Uetsuka H and Onishi H 2004 *Jpn. J. Appl. Phys.* **43** 4647

[23] Okamoto K, Yoshimoto K, Sugawara Y and Morita S 2003 *Appl. Surf. Sci.* **210** 128

[24] Shiota T and Nakayama K 2002 *Jpn. J. Appl. Phys.* **41** L1178

[25] Onishi H, Fukui K and Iwasawa Y 1995 *Bull. Chem. Soc. Jpn*. **68** 2447

[26] Sasahara A, Pang C L and Onishi H 2006 *J. Phys. Chem. B* **110**, 17584

[27] Gan S, Liang Y, Baer D R and Grant A W 2001 *Surf. Sci.* **475** 159

[28] Dulub O, Hebenstreit W and Diebold U 2000 *Phys. Rev. Lett.* **84** 3646

[29] Onishi H, Aruga T, Egawa C and Iwasawa Y 1988 *Surf. Sci.* **193** 33

[30] Lide D R (ed) *CRC Handbook of Chemistry and Physics* 2004 (Boca Raton FL: CRC Press)

[31] Sasahara A, Uetsuka H and Onishi H 2001 *Phys. Rev. B* **64** 121406

[32] Jensen M B, Myler U and Thiel P A 1993 *Surf. Sci.* **290** L655

[33] Gao Q and Hemminger J C 1991 *Surf. Sci.* **248** 45

[34] Carrara M, Nüesch F and Zuppiroli L 2001 *Synth. Met*. **121** 1633

[35] Hlavathy Z and Tétényi P 1998 *Surf. Sci.* **410** 39

[36] Wintterlin J, Völkening S, Janssens T V W, Zambelli T and Ertl G 1997 *Science* **278** 1931

[37] Fisher G B and Gland J L 1980 *Surf. Sci.* **94** 446

[38] Shern C S 1992 *Surf. Sci.* **264** 171

[39] Christmann K, Ertl G and Pignet T 1976 *Surf. Sci.* **54** 365

Figure captions

Figure 1. A model of the TiO_2(110)-(1×1) surface. Small and large spheres represent Ti and O atoms, respectively. The O atoms are shaded according to depth. Six pivalate molecules are anchored to the lower terrace in a (2×1) periodicity.

Figure 2. Constant current images of TiO_2(110) surfaces (20×20 nm^2). (a) (1×1) surface. Sample bias voltage (V_s) = +1.0 V, tunneling current (I_t) = 1.0 nA. (b) Low Pt-loaded surface. V_s = +1.3 V, I_t = 1.0 nA. (c) High Pt-loaded surface. V_s = +1.4 V, I_t = 1.0 nA. (d) Low Pt-loaded surface after pivalate adsorption. V_s = +0.9 V, I_t = 1.0 nA. (e) High Pt-loaded surface after pivalate adsorption. V_s = +1.0 V, I_t = 1.0 nA (inset: 4×4 nm^2, V_s = +1.0 V, I_t = 1.0 nA). (f) Low Pt-loaded surface after photodecomposition of the pivalates. V_s = +0.9 V, I_t = 1.0 nA. (g) High Pt-loaded surface after photodecomposition of the pivalates. V_s = +1.4 V, I_t = 1.0 nA (inset: 4×4 nm^2, V_s = +1.2 V, I_t = 1.0 nA).

Figure 3. Topography (left column) and work function map (right column) of the (a) low Pt-loaded surface and (b) high Pt-loaded surface (30×30 nm^2). Positions of some Pt clusters are indicated by arrowhead. (a) Frequency shift (Δf) = -141 Hz, peak-to-peak amplitude of the cantilever oscillation ($A_{p\text{-}p}$) = 7.0 nm, scanning speed (v_s) = 1.7 s/pixel. (b) Δf = - 69 Hz, $A_{p\text{-}p}$ = 6.9 nm, v_s = 1.7 s/pixel. (c) Schematic model of the work function perturbation on the surface. (d) Work function difference between the Pt clusters and surrounding TiO_2 surfaces plotted as a function of the cluster-substrate interface area. Open circles: low-loaded surfaces. Solid circles: high-loaded surfaces.

Figure 4. Topography (left column) and work function map (right column) obtained after pivalate adsorption on the (a) low Pt-loaded surface and (b) high Pt-loaded surface (30×30 nm^2). Positions of some Pt clusters are indicated by arrowhead. (a) Δf = -127 Hz, $A_{p\text{-}p}$ = 6.8 nm, v_s = 3.3 s/pixel. (b) Δf = -52 Hz, $A_{p\text{-}p}$ = 6.7 nm, v_s = 3.3 s/pixel. (c) Schematic model of the work function perturbation on the surface. Dotted lines show work function perturbation on a pivalate-free surface. (d) Work function difference between the Pt clusters and the surrounding pivalate-covered TiO_2 surface plotted as a function of the

cluster-substrate interface area. Open circles: low-loaded surfaces. Solid circles: high-loaded surfaces.

Figure 5. Topography (left column) and work function map (right column) obtained after photodecomposition of the pivalates on the (a) low Pt-loaded surface and (b) high Pt-loaded surface (30×30 nm^2). Positions of some Pt clusters are indicated by arrowhead. (a) Δf = -47 Hz, $A_{p\text{-}p}$ = 7.0 nm, v_s = 3.3 s/pixel. (b) Δf = -41 Hz, $A_{p\text{-}p}$ = 6.7 nm, v_s = 1.7 s/pixel. (c) Schematic model of the work function perturbation on the surface. Dotted lines show work function perturbation on a pivalate-covered surface before UV irradiation. (d) Work function difference between the Pt clusters and the surrounding pivalate-covered TiO_2 surface plotted as a function of the cluster-substrate interface area. Open circles: low-loaded surfaces. Solid circles: high-loaded surfaces.

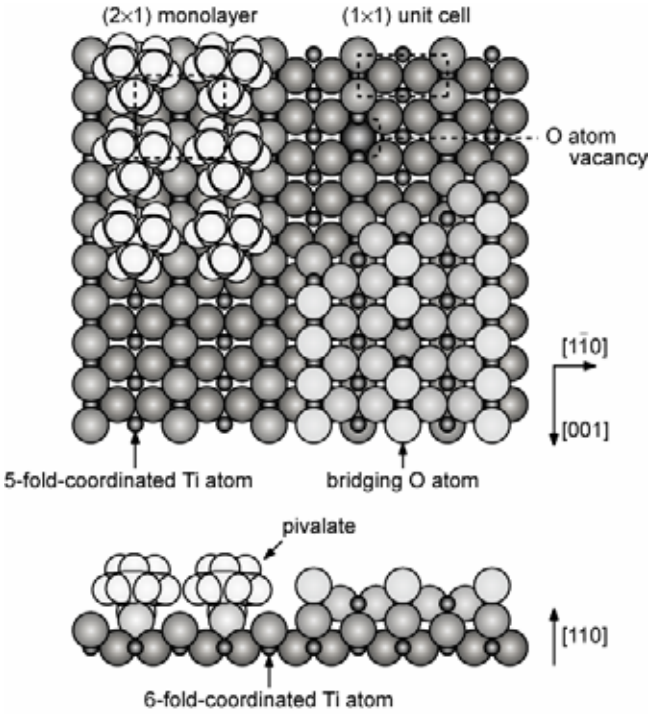

Figure 1 Hiehata et al.

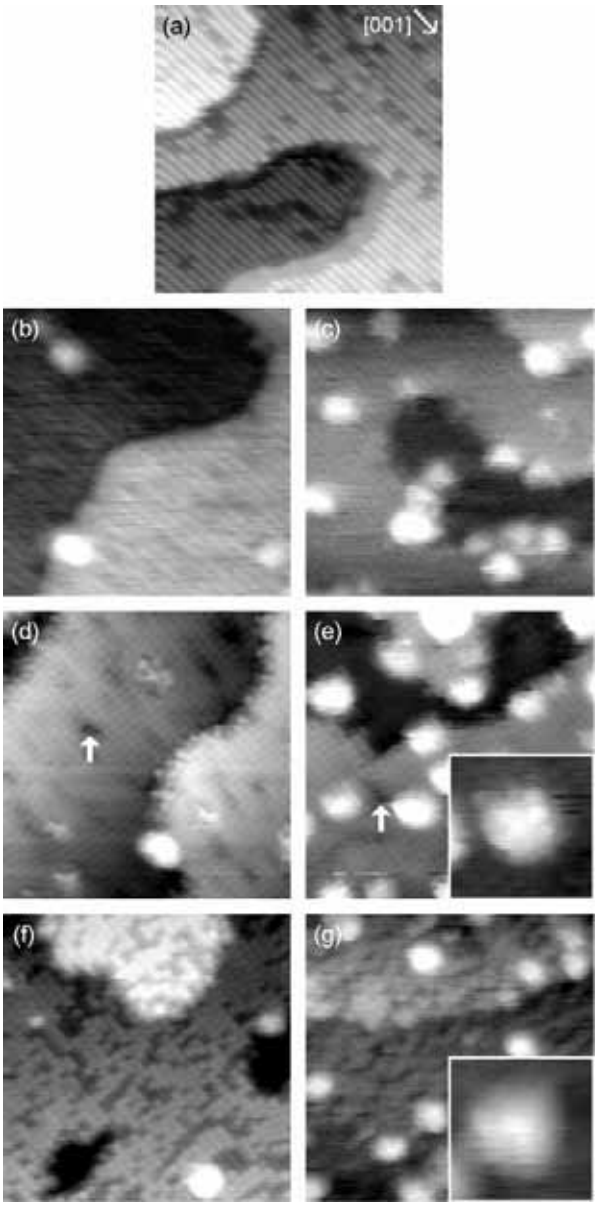

Figure 2 Hiehata et al.

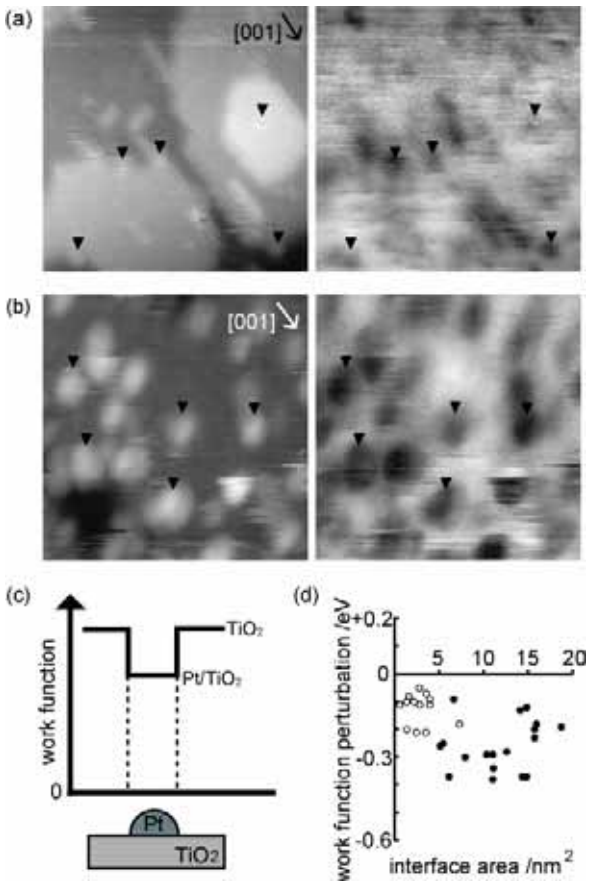

Figure 3 Hiehata et al.

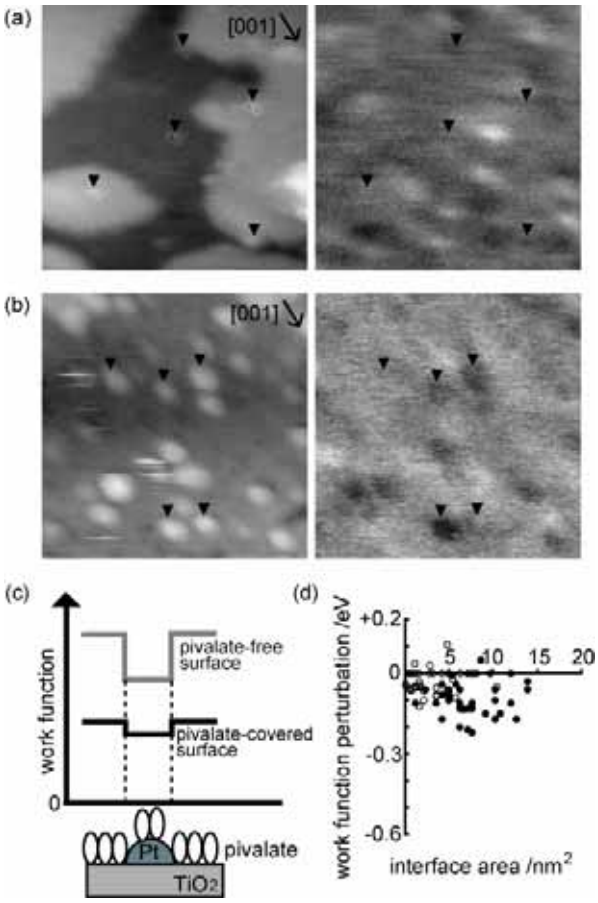

Figure 4 Hiehata et al.

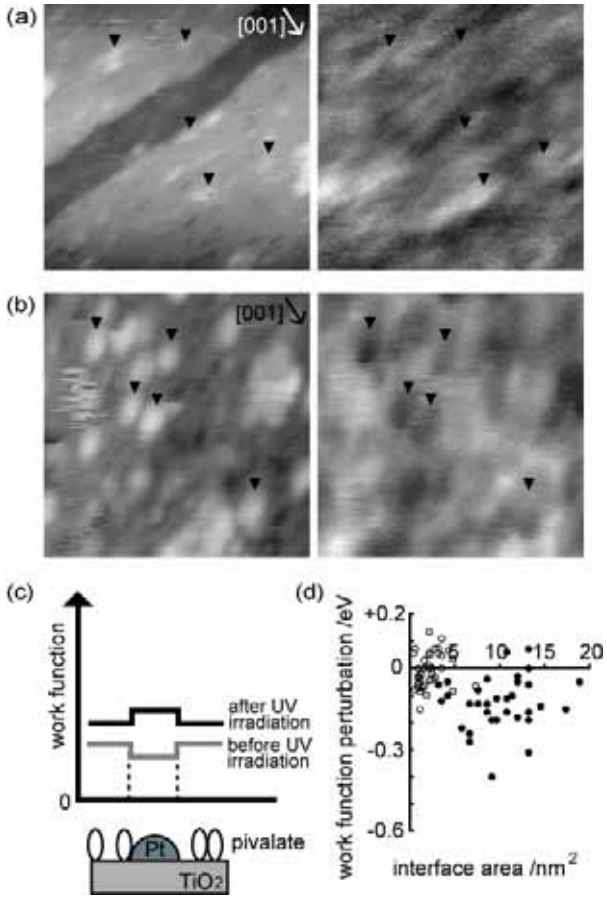

Figure 5 Hiehata et al.